



Response of porous SMA: a micromechanical study

V. Sepe, S. Marfia

University of Cassino and Southern Lazio

v.sepe@unicas.it, marfia@unicas.it

F. Auricchio

University of Pavia

auricchio@unipv.it

ABSTRACT. Lately porous shape memory alloys (SMA) have attracted great interest as low weight materials characterized by high energy dissipation capability. In the present contribution a micromechanical study of porous SMA is proposed, introducing the simplifying hypothesis of periodic distribution of voids. The mechanical response of the heterogeneous porous medium is derived by performing nonlinear finite element micromechanical analyses considering a typical repetitive unit cell made of a circular hole in a dense SMA matrix and prescribing suitable periodicity and continuity conditions. The constitutive behavior and the dissipation energy capability of the porous Nitinol are examined for several porosity levels. Numerical applications are performed in order to test the ability of the proposed procedure to well capture the overall behavior and the key features of the special heterogeneous material.

KEYWORDS. Shape Memory Alloys; Porous material; Micromechanics; Dissipation.

INTRODUCTION

Shape Memory Alloys (SMA) are characterized by a very special behavior due to their capability to undergo reversible changes of the crystallographic structure, depending on the temperature and on the stress state. These changes can be interpreted as reversible martensitic transformations between a crystallographic more-ordered parent phase, the austenite, and a crystallographic less-ordered product phase, the martensite. Thanks to their unique properties over the last decades SMA have been used for a large number of applications in several engineering fields, from aerospace to medical device industries.

Recently, driven by biomedical applications, a great interest has arisen concerning a particular class of SMA: the porous SMA. Currently, several methods are adopted for manufacturing porous SMA from elemental powders. Many porous NiTi SMA with different structures of pores have been successfully produced by sintering at elevated pressure via a hot isostatic press or metal injection molding [1], spark plasma sintering [2], combustion synthesis with a self-propagating wave [3].

The possibility of producing SMA in porous form has opened new fields of applications owing to their low-weight with high energy dissipation properties. Porous shape memory alloys combine benefits from dense SMA and porous structure. In fact, even beyond the shape memory characteristics, porous SMA with a relatively low density can enlarge the applicability of dense SMA. In addition to the large recoverable strains observed by SMA, the porous counterpart offers



the possibility of undergoing greater overall strains as well as higher specific energy absorption under dynamic loading conditions due to the possibility of wave scattering.

In the biomedical field, thanks to their high biocompatibility [4] and their capacity to exhibit high strength, NiTi foams have been tested as bone implant materials [5], effectively exhibiting a considerable amount of bone ingrowth. In particular, these materials display unique characteristics such as: relatively low stiffness, useful to minimize stress shielding phenomenon, shape recovery effect, that facilitates implant insertion and ensures good mechanical stability within the host tissue, elevated osteoconductivity and better osseointegration and osteoconductivity than bulk NiTi alloys.

In the last years, applications of porous SMA in the field of Civil and Mechanical Engineering have also been considered. The potential applications of porous SMA exploit their ability to carry significant loads and their high energy absorption capability. In fact, the porous SMA shows a higher specific damping capacity under dynamic loading conditions with respect to the dense SMA, because the pores facilitate an additional absorption of the impact energy.

In order to correctly reproduce the behavior of the porous SMA, the development of accurate models describing their properties is needed. Several papers have been published concerning the modeling of porous SMA (e.g. [6-8]).

The porous SMA material can be treated as a composite with SMA as the matrix and pores as the inclusions. In order to derive the mechanical response of porous SMA, micromechanical averaging techniques have been developed in the available literature, as for instance [9, 10].

Indeed, different micromechanical and homogenization techniques, usually applied to study composites can be used to model porous SMA, such as the Eshelby dilute inclusion technique or the Mori-Tanaka scheme [11, 12] or the self-consistent method. An interesting approach that has been adopted to study the behavior of porous materials is based on the assumption of having a periodic distribution of pores. In this case, the problem can be solved by using a computational homogenization technique based, for instance, on nonlinear finite element analyses of a single unit cell with suitable boundary conditions.

The behavior of porous SMA under cyclic loading conditions has been studied in [13], where the constitutive law has been enhanced to account for the development of permanent inelastic strains due to stress concentrations in the porous microstructure.

Aim of the present contribution is to propose a micromechanical study of porous SMA. In particular, the response of porous SMA is derived by performing the nonlinear finite element micromechanical analysis for the typical repetitive unit cell, considering periodicity conditions. The constitutive model, proposed in [15] and [16] and able to reproduce the main properties of dense shape memory alloys response, is adopted in order to simulate the behavior of the porous SMA.

The constitutive response and the dissipation energy capability of the porous Nitinol are investigated for several values of porosity. Numerical applications are developed in order to assess the ability of the presented procedure to well capture the overall behavior of the special heterogeneous material, correctly reproducing the pseudoelastic effect, a key feature of the shape memory alloys.

POROUS SMA MODELING

The porous SMA is a composite material in which voids can be considered as inclusion in a dense SMA matrix. The study of the mechanical response of porous SMA can be conducted performing micromechanical analyses which accounts for the presence of a random distribution of voids characterized by different shape and dimensions.

In this study, developed in the framework of small strains, the simplifying hypothesis of regular, i.e. periodic, distribution of voids is introduced: in other words, it is assumed that all the voids have the same dimension and shape. In such a way, the study can be limited to the analysis of a unit cell (UC) which is representative of the heterogeneous material and that completely accounts for the geometry and material properties of the constituents of the composite.

Such a simplified approach allows to derive the influence of the void volume fraction on the mechanical response.

SMA constitutive model

Concerning the modeling of dense SMA material, the model initially proposed by Souza et al. [14] and modified first by Auricchio and Petri [15] and, then, by Evangelista et al. [16] is adopted to reproduce the shape memory alloys behavior. In the following discussion, the Voigt notation is adopted, so that second order tensors are represented as vectors and fourth order tensors as matrices. In particular, the strains and the stresses are reported as vectors with 6 components, while symmetric 6×6 matrix defines the elastic constitutive matrix. The use of this notation is preferred as it enables a straightforward implementation in a numerical code.



The model is thermodynamically consistent and it assumes the total strain $\boldsymbol{\varepsilon}$ and the absolute temperature T as control variables and the transformation strain vector \mathbf{d} as internal variable. The transformation strain \mathbf{d} describes the strain associated to the phase transformation and, in particular, to the conversion from austenite or multivariant martensite to single-variant martensite. The norm of \mathbf{d} , denoted as η , is constrained to satisfy the inequalities $0 \leq \eta \leq \varepsilon_L$, where ε_L is a material parameter indicating the maximum transformation strain reached at the end of the conversion from austenite or multivariant martensite to single-variant martensite, during a uniaxial test.

According to the thermodynamic formulation, the existence of a thermodynamic potential is postulated and a free specific energy function is introduced through a convex potential as:

$$\Psi(\boldsymbol{\varepsilon}, \mathbf{d}, T) = \Psi_e(\boldsymbol{\varepsilon}, \mathbf{d}, T) + \Psi_p(\mathbf{d}, T) + \Psi_{id}(T) \quad (1)$$

where: Ψ_e represents the elastic strain energy due to the thermo-elastic material deformations, depending on the total strain $\boldsymbol{\varepsilon}$, on the inelastic strain \mathbf{d} and on the absolute temperature T ; Ψ_p is the inelastic energy which accounts for all the inelastic phenomena and that is related to the internal variable \mathbf{d} and to the absolute temperature T ; Ψ_{id} is defined as the free energy due to the change in temperature with respect to the reference state for an incompressible ideal solid [14, 15, 16].

In particular, the thermo-elastic potential Ψ_e is defined as:

$$\Psi_e(\boldsymbol{\varepsilon}, \mathbf{d}, T) = \frac{1}{2}(\boldsymbol{\varepsilon} - \mathbf{d})^T \mathbf{C}(\boldsymbol{\varepsilon} - \mathbf{d}) \quad (2)$$

where \mathbf{C} is the elasticity constitutive matrix and the superscript T denotes the transposition operation.

The inelastic potential in the dense SMA is set as proposed in [16] and it is function of the temperature and the transformation strain \mathbf{d} :

$$\Psi_p(\mathbf{d}, T) = \beta \langle T - M_f \rangle \eta + \frac{1}{2} b \eta^2 + \mathcal{I}_{\varepsilon_L}(\eta) \quad (3)$$

where:

- β is a material parameter linked to the dependence of the transformation stress threshold on the temperature;
- M_f represents the finishing temperature of the austenite-martensite phase transformation evaluated at a stress free state;
- the symbol $\langle \bullet \rangle$ indicates the positive part of the argument;
- $\eta = \sqrt{\mathbf{d}^T \mathbf{M}^V \mathbf{d}}$ with

$$\mathbf{M}^V = \begin{bmatrix} \mathbf{I} & \mathbf{0} \\ \mathbf{0} & \frac{1}{2} \mathbf{I} \end{bmatrix} \quad (4)$$

\mathbf{I} and $\mathbf{0}$ being the 3×3 identity and zero matrices, respectively;

- b is a material parameter associated to the slope of the linear relation ruling the value of the transformation stress threshold with the temperature in the uniaxial case;
- $\mathcal{I}_{\varepsilon_L}(\eta)$ is the indicator function introduced in order to satisfy the fulfillment of the constraint on the transformation strain norm:

$$\mathcal{I}_{\varepsilon_L}(\eta) = \begin{cases} 0 & \text{if } \eta \leq \varepsilon_L \\ +\infty & \text{if } \eta > \varepsilon_L \end{cases} \quad (5)$$

which ensures that the norm of the transformation strain has to be bounded between zero, for the case of a material without oriented martensite, and the maximum value ε_L , for the case in which the material is fully transformed in single-variant oriented martensite.

The state laws can be derived as:



$$\boldsymbol{\sigma} = \frac{\partial \Psi}{\partial \boldsymbol{\varepsilon}} \tag{6}$$

$$\mathbf{X} = -\frac{\partial \Psi}{\partial \mathbf{d}} \tag{7}$$

which define the thermoelastic laws for the stress and the thermodynamic force, respectively.

The latter quantity \mathbf{X} represents the thermodynamic variable associated with the transformation strain and it is indicated as the transformation stress. The Eq. (6) and (7) state that $\boldsymbol{\sigma}$ and \mathbf{X} are the quantities thermodynamically conjugated to the deformation-like variables $\boldsymbol{\varepsilon}$ and \mathbf{d} , respectively. Therefore, the state laws assume the expressions:

$$\boldsymbol{\sigma} = \mathbf{C}(\boldsymbol{\varepsilon} - \mathbf{d}) \tag{8}$$

$$\mathbf{X} = \boldsymbol{\sigma} - [\beta \langle T - M_f \rangle + b\eta + \gamma] \frac{\partial \eta}{\partial \mathbf{d}} \tag{9}$$

where γ is an element of the subdifferential of the indicator function $\mathcal{I}_{\varepsilon_L}(\eta)$ which results as:

$$\gamma \in \partial \mathcal{I}_{\varepsilon_L}(\eta) = \begin{cases} 0 & \text{if } \eta < \varepsilon_L \\ \mathcal{R}^+ & \text{if } \eta = \varepsilon_L \\ \emptyset & \text{if } \eta > \varepsilon_L \end{cases} \tag{10}$$

Eq. (9) can be rewritten in the following form:

$$\mathbf{X} = \boldsymbol{\sigma} - \boldsymbol{\alpha} \tag{11}$$

with $\boldsymbol{\alpha}$ playing a role similar to the back stress in the classical plasticity theory with kinematic hardening; it is defined as:

$$\boldsymbol{\alpha} = [\beta \langle T - M_f \rangle + b\eta + \gamma] \frac{\partial \eta}{\partial \mathbf{d}} \tag{12}$$

resulting a linear function of the temperature when $T \geq M_f$.

The yield function is assumed to depend on the deviatoric part of the thermodynamic force and it is introduced as:

$$F(\mathbf{X}^d) = \sqrt{2J_2(\mathbf{X}^d)} - R \tag{13}$$

where:

- R represents the radius of the elastic domain in the deviatoric space, given by the relation:

$$R = \sqrt{\frac{2}{3}} \sigma_t \tag{14}$$

with σ_t the uniaxial critical stress evaluated at $T \leq M_f$;

- \mathbf{X}^d is the deviatoric part of the associated variable \mathbf{X} and it is computed as:

$$\mathbf{X}^d = \mathbf{I}^{dev} \mathbf{X} \tag{15}$$

where:

$$\mathbf{I}^{dev} = \begin{bmatrix} \mathbf{Dev} & \mathbf{0} \\ \mathbf{0} & \mathbf{I} \end{bmatrix} \quad \text{with} \quad \mathbf{Dev} = \begin{bmatrix} 2/3 & -1/3 & -1/3 \\ -1/3 & 2/3 & -1/3 \\ -1/3 & -1/3 & 2/3 \end{bmatrix} \tag{16}$$

- J_2 is the second invariant of \mathbf{X}^d determined through the following formula:

$$J_2 = \frac{1}{2} [(\mathbf{X}^d)^T \mathbf{M}^S \mathbf{X}^d] \quad \text{with} \quad \mathbf{M}^S = \begin{bmatrix} \mathbf{I} & \mathbf{0} \\ \mathbf{0} & 2\mathbf{I} \end{bmatrix} \tag{17}$$



The equation describing the associative normality rule for the internal variable \mathbf{d} is:

$$\dot{\mathbf{d}} = \dot{\zeta} \frac{\partial F(\mathbf{X}^d)}{\partial \mathbf{X}} \quad (18)$$

with $\dot{\zeta}$ the plastic multiplier. From the analysis of the flow rule form it can be noted that the transformation strain \mathbf{d} is a deviator vector and, thus, the condition of incompressibility during the inelastic flow is recovered. The model is completed introducing the classical Kuhn-Tucker conditions:

$$\dot{\zeta} \geq 0 \quad F \leq 0 \quad \dot{\zeta} F = 0 \quad (19)$$

that reduce the problem to a constrained optimization problem. The normality properties are sufficient to guarantee the satisfaction the second principle of thermodynamics in the form of the Clausius-Duhem inequality [17]. Thus, the proposed model results to be consistent with the thermodynamic formulation.

Periodic microstructure

The periodic microstructure of the analyzed material allows to consider a repetitive unit cell (UC) subjected to suitable boundary conditions in order to determine the overall behavior of the whole heterogeneous material.

In the following, the UC, composed of the SMA matrix and the pore, is denoted as Ω and the discussion is limited to the framework of 2D plane strain problems.

The components of the 2D macroscopic fields of the average strain vector $\bar{\boldsymbol{\varepsilon}} = \{\bar{\boldsymbol{\varepsilon}}_{11} \quad \bar{\boldsymbol{\varepsilon}}_{22} \quad \bar{\boldsymbol{\gamma}}_{12}\}^T$ and of the average stress vector $\bar{\boldsymbol{\sigma}} = \{\bar{\boldsymbol{\sigma}}_{11} \quad \bar{\boldsymbol{\sigma}}_{22} \quad \bar{\boldsymbol{\sigma}}_{12}\}^T$ can be defined in Ω , respectively, as:

$$\bar{\boldsymbol{\varepsilon}} = \frac{1}{V} \int_{\partial\Omega} \begin{bmatrix} n_1 & 0 \\ 0 & n_2 \\ n_2 & n_1 \end{bmatrix} \mathbf{u} dA, \quad \bar{\boldsymbol{\sigma}} = \frac{1}{V} \int_{\partial\Omega} \begin{bmatrix} x_1 & 0 \\ 0 & x_2 \\ x_2 & x_1 \end{bmatrix} \mathbf{t} dA \quad (20)$$

where $\mathbf{n}(\mathbf{x})$ represents the normal to the boundary of the unit cell $\partial\Omega$, $\mathbf{u}(\mathbf{x})$ is displacement vector and $\mathbf{t}(\mathbf{x})$ is the

traction vector defined as $\mathbf{t} = \begin{bmatrix} n_1 & 0 & n_2 \\ 0 & n_2 & n_1 \end{bmatrix} \begin{Bmatrix} \boldsymbol{\sigma}_{11} \\ \boldsymbol{\sigma}_{22} \\ \boldsymbol{\sigma}_{12} \end{Bmatrix}$.

In the presence of pores the average strain and stress fields take the following form:

$$\bar{\boldsymbol{\varepsilon}} = \frac{1}{V} \int_{\Omega} \boldsymbol{\varepsilon} dV - \frac{1}{V} \int_{\partial H} \begin{bmatrix} n_1 & 0 \\ 0 & n_2 \\ n_2 & n_1 \end{bmatrix} \mathbf{u} dA, \quad \bar{\boldsymbol{\sigma}} = \frac{1}{V} \int_{\Omega} \boldsymbol{\sigma} dV \quad (21)$$

where ∂H is the union of the surfaces of voids present in the UC made of porous material. In Eq. (21)₂ the term:

$$-\frac{1}{V} \int_{\partial H} \begin{bmatrix} x_1 & 0 \\ 0 & x_2 \\ x_2 & x_1 \end{bmatrix} \mathbf{t} dA$$

has not been reported, since pores are considered regions with null tractions and at the interfaces

∂H the continuity of the tractions has to be ensured.

For periodic media, introducing a Cartesian reference system (O, x_1, x_2) in the UC, the displacement field $\mathbf{u} = \{u_1 \quad u_2\}^T$

in the typical point $\mathbf{x} = \{x_1 \quad x_2\}^T$ of the unit cell is given by the relations:

$$\begin{aligned} u_1 &= \bar{\boldsymbol{\varepsilon}}_{11} x_1 + \frac{1}{2} \bar{\boldsymbol{\gamma}}_{12} x_2 + \tilde{u}_1, \\ u_2 &= \frac{1}{2} \bar{\boldsymbol{\gamma}}_{12} x_1 + \bar{\boldsymbol{\varepsilon}}_{22} x_2 + \tilde{u}_2, \end{aligned} \quad (22)$$



where $\bar{\varepsilon}_{11}$, $\bar{\varepsilon}_{22}$ and $\bar{\gamma}_{12}$ are the components of $\bar{\boldsymbol{\varepsilon}}$, the effective strain acting on the UC; \tilde{u}_1 and \tilde{u}_2 are the components of $\tilde{\mathbf{u}}(\mathbf{x})$, the vector representing the periodic part of the displacement. From formula (22), the total strain in the typical point \mathbf{x} of the unit cell is given by:

$$\boldsymbol{\varepsilon}(\mathbf{x}) = \bar{\boldsymbol{\varepsilon}} + \tilde{\boldsymbol{\varepsilon}}(\mathbf{x}) \quad (23)$$

where $\tilde{\boldsymbol{\varepsilon}}(\mathbf{x})$ represents the periodic part of the strain, characterized by null average in Ω and associated to the periodic displacement $\tilde{\mathbf{u}}(\mathbf{x})$. As suggested in [18, 9], for rectangular 2D unit cells with the total dimensions along the two coordinate axes x_1, x_2 denoted by $2a_1$ and $2a_2$, the classical periodicity conditions:

$$\begin{aligned} \tilde{u}_i(a_1, x_2) &= \tilde{u}_i(-a_1, x_2) \quad \forall x_2 \in [-a_2, a_2] \\ \tilde{u}_i(x_1, a_2) &= \tilde{u}_i(x_1, -a_2) \quad \forall x_1 \in [-a_1, a_1] \end{aligned} \quad (24)$$

have to be prescribed to the displacement field, being $i = 1, 2$.

NUMERICAL RESULTS

In the following numerical applications 2D micromechanical analyses are developed in order to study the overall mechanical response of periodic porous shape memory alloys and to investigate the influence of the volume fraction of voids on their mechanical behavior.

A square periodic UC made of a circular hole embedded in a dense Nitinol matrix is analyzed. The constituent material properties adopted for the dense SMA matrix are set as in [16] and are defined in Tab. 1, where the symbols E and ν indicate the Young modulus and the Poisson ratio, respectively.

<i>NiTi mechanical properties</i>	
$E = 53000 \text{ MPa}$	$\nu = 0.36$
$b = 1000 \text{ MPa}$	$\beta = 2.1 \text{ MPaK}^{-1}$
$\varepsilon_L = 0.06$	$M_f = 223 \text{ K}$
$\sigma_i = 61.23 \text{ MPa}$	

Table 1: Material properties for the porous NiTi SMA.

Fig. 1 shows the UC geometry where a unit thickness is considered.

Different volume fractions of voids are analyzed keeping constant the side l of the UC and varying the radius R of the pore. In particular six UCs are examined with different values of porosity set as: 5%, 10%, 20%, 35%, 45% and 55%.

The mechanical response of the heterogeneous media, when the pseudoelastic effect is activated, is investigated.

In fact, an increasing value of the average strain $\bar{\varepsilon}_{11}$ is prescribed in the UCs until the value $\bar{\varepsilon}_{11} = 0.02$ is reached at a constant temperature $T = 270 \text{ K}$, greater than A_f , temperature at which the more-ordered austenitic phase is stable.

Then, the prescribed strain is removed allowing the recovery of the transformation strain in the porous SMA, exploiting the NiTi pseudoelasticity.

The described loading history is prescribed on the six unit cells characterized by the different volume fractions of voids and on a UC made of homogeneous material (0% porosity) with the same mechanical properties defined in Tab. 1. Fig. 2 shows the behavior of the unit cells in terms of the average normal stress $\bar{\sigma}_{11}$ versus the average strain $\bar{\varepsilon}_{11}$ for all the different analyses characterized by the different volume of voids (denoted in the legend with the acronym Vv).

Then, the same loading history is assigned on the considered unit cells, but prescribing a higher value of the average normal strain $\bar{\varepsilon}_{11}$ at the end of the loading phase, up to 4%. The mechanical responses of the porous SMA cells with



different porosities are illustrated in Figure 3, where the average normal stress versus the average normal strain along the x_1 -direction is plotted.

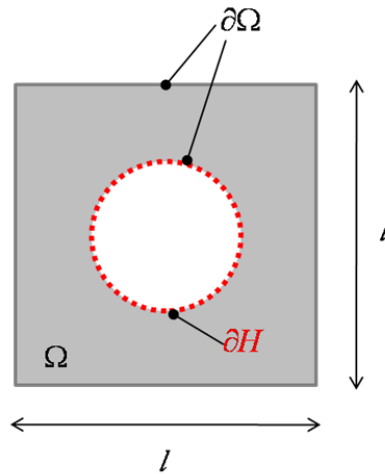


Figure 1: Porous NiTi SMA periodic unit cell.

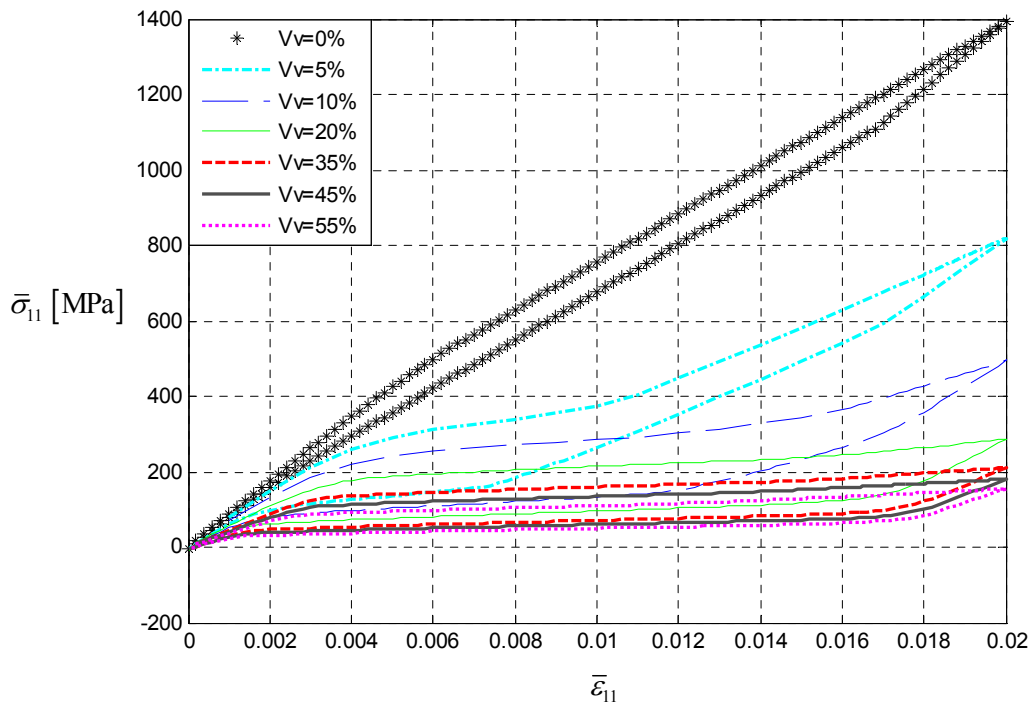


Figure 2: Mechanical responses of the porous UCs along x_1 -direction for the first loading history.

From Fig. 2 and Fig. 3 it can be pointed out that the constitutive model adopted to reproduce the porous SMA response is able to correctly capture the pseudoelastic effect for both the loading histories characterized by different values of the maximum average strain prescribed at the end of the loading phase.

It can be observed that for the homogeneous SMA specimen with no pores (Fig. 2 and Fig. 3) the stress-strain slope occurring during transformation is rather high due to the fact that the analyses are performed under plane strain conditions.

Moreover it can be remarked that for both the loading histories the value of the maximum average normal stress along the x_1 -direction ($\bar{\sigma}_{11}^{\max}$), reached at the end of the loading step, decreases for increasing values of porosity.



The results obtained by the adopted micromechanical approach underline that both the stress-strain slope during transformation and the yield strength significantly reduce with the increase in porosity. These outcomes are well supported and justified by a large amount of experimental data, such as the ones provided in [11, 20-24] for porous shape memory alloys.

Fig. 4 shows the trend of the maximum value of the average normal stress along x_1 -direction achieved for the different volume fractions of voids. In particular, a comparison between the results obtained for the first loading history ($\bar{\epsilon}_{11} = 2\%$) and denoted with the triangle marker, and the results provided by the second loading history ($\bar{\epsilon}_{11} = 4\%$) and indicated with the round symbol, is given. It can be noted that being equal the volume fraction of voids, the value of the maximum average tensile stress is obviously higher for the analyses in which the average strain reaches the value of $\bar{\epsilon}_{11} = 0.04$.

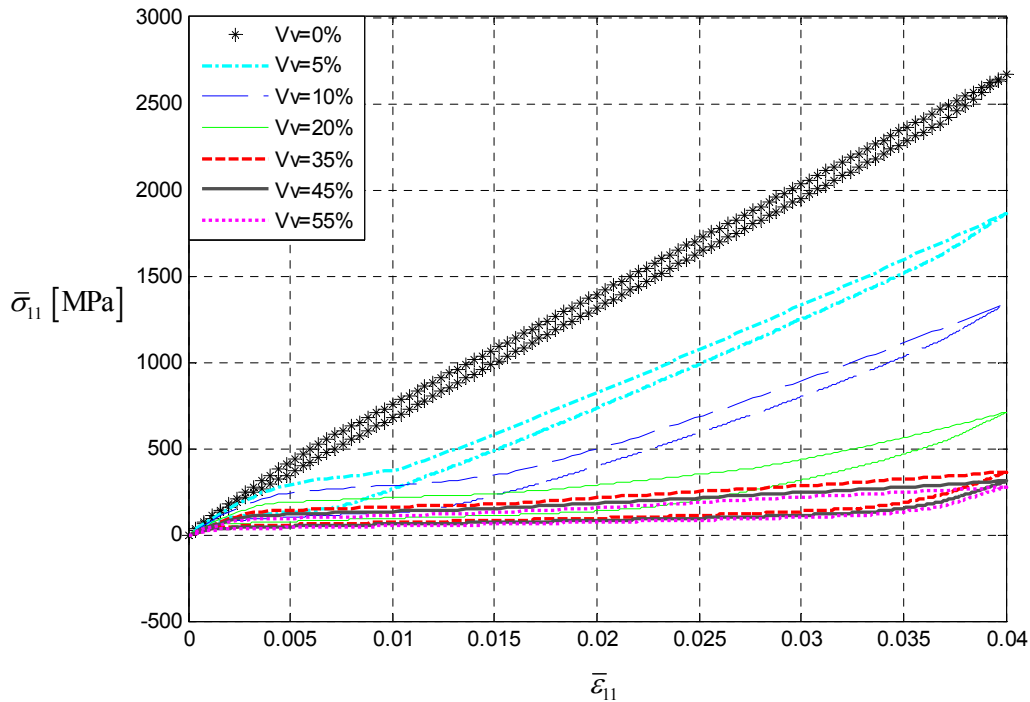


Figure 3: Mechanical responses of the porous UCs along x_1 -direction for the second loading history.

However the difference between the values of $\bar{\sigma}_{11}^{\max}$ for the two loading histories tends to decrease with the increasing of porosity, so that for a high level of voids fraction the increase of the average strain leads to a low increase of the maximum tensile average stress.

The energy dissipation capability of the porous NiTi, due to the stress hysteresis based on the pseudoelastic properties, has also been investigated for the considered unit cells and for both the loading histories. In Fig. 5 the ratio between the dissipated energy and the volume of the solid fraction is plotted in function of the porosity for the two loading paths.

The comparison between the results obtained by the two loading cases shows that the higher is the level of the prescribed average strain on the UCs, the higher is the energy dissipated by the porous SMA in relation to its own weight.

It can be put in evidence that for the first loading history the energy dissipated per solid volume during the pseudoelastic loading cycle increases with the increasing of the porosity level until the volume fraction of voids is equal to 20%. As the value of the volume of voids continues to increase, the dissipated energy tends to keep almost constant, with a value that is higher than the one obtained for the case of homogeneous shape memory alloys. Furthermore, for the second loading history characterized by a maximum value of average strain up to 4%, it can be underlined that the energy dissipation capability increases in function of the volume fraction of voids, providing the maximum value for the case of porosity equal to 55%.

Thus the performed analyses show that the energy dissipation capability of porous materials is obviously influenced by the entity of the prescribed loading strain. Moreover it can be remarked that high levels of volume fraction of voids can lead



to a heterogeneous material able to dissipate more than shape memory alloys characterized by low porosity or dense material.

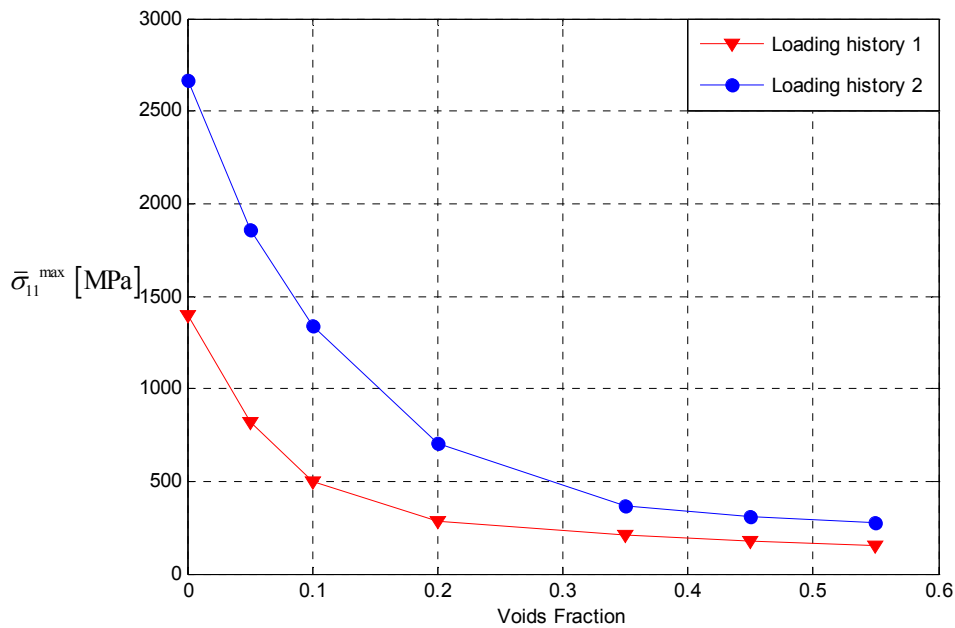


Figure 4: Maximum average normal stress for the considered porosities provided by the two loading histories.

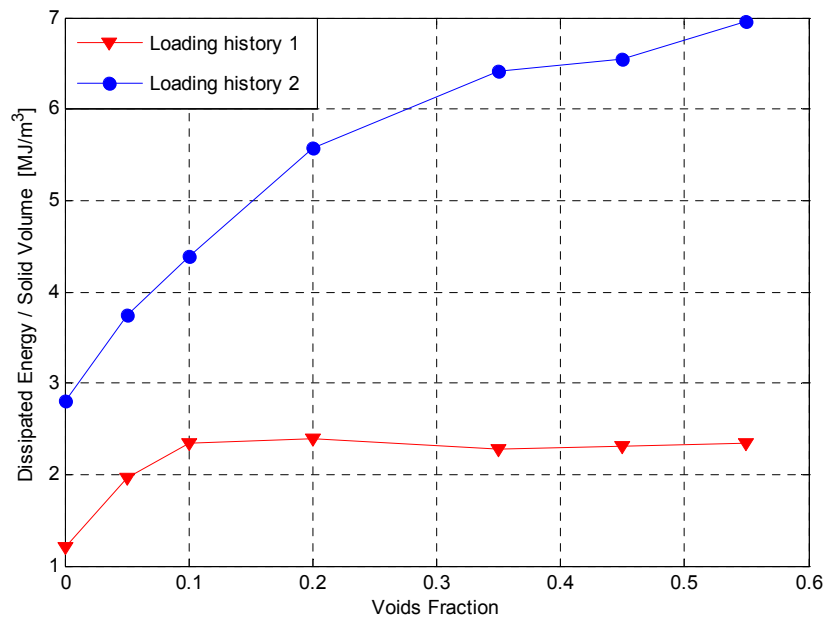


Figure 5: Dissipated energy per solid volume for the considered porosities provided by the two loading histories.

CONCLUSIONS

The mechanical behavior of porous SMA has been investigated in the present work. The simplifying hypothesis of considering a periodic distribution of voids all characterized by the same shape and dimensions has been assumed so that a typical repetitive unit cell, representative of the heterogeneous material and able to account for the properties of the composite medium, has been analyzed. The model proposed by [15] and [16] for dense SMA has been adopted to reproduce the constitutive behavior of porous shape memory alloys.



Plane strain 2D micromechanical analyses have been developed to derive the influence of the volume fraction of voids on the mechanical response of the porous NiTi. In particular, the behavior of the heterogeneous material when the pseudoelastic effect is activated, has been investigated considering different periodic unit cells characterized by several values of porosity. The performed analyses have shown the ability of the adopted constitutive model to reproduce the pseudoelastic effect for porous SMA.

Moreover the influence of the volume of voids on the maximum tensile stresses reached by the porous material and on the energy dissipation capability has been examined for two different values of prescribed average strain. The obtained results have demonstrated that the value of the maximum average normal stresses reached during the loading phase decreases for increasing values of porosity and that for a high level of the volume fraction of voids the increase of the prescribed average strain leads to a low increase of the maximum value of the tensile average stress.

Furthermore, analyzing the dissipation capability of the porous medium during the pseudoelastic loading cycle, the developed analyses have put in evidence that the higher is the porosity level the higher is the capability of the porous SMA to dissipate energy in relation to its own weight. Thus the attractive feature of low-weight with high energy dissipation of the porous shape memory alloys is well captured by the proposed simplified micromechanical approach.

Future developments will be focused on other particular porous SMA issues, such as the presence of pores with different shapes and of interconnected pores or the possible presence of porous internal pressure, relevant for the case of smart biomedical applications. Moreover an extension of the analyses to the finite strain regime will be considered in future works in order to account also for the variation of the pore shape during the loading histories.

ACKNOWLEDGEMENT

The financial supports of PRIN 2010-11, project "Advanced mechanical modeling of new materials and technologies for the solution of 2020 European challenges" CUP n. F11J12000210001 are gratefully acknowledged. The authors wish to thank Prof. Elio Sacco for his useful comments and suggestions.

REFERENCES

- [1] Krone, L., Schüller, E., Bram, M., Hamed, O., Buchkremer, H.P., Stöver, D., Mechanical behaviour of NiTi parts prepared by powder metallurgical methods. *Mater. Sci. Eng. A*, 378 (2004) 185–190.
- [2] Shearwood, C., Fu, Y.Q., Yu, L., Khor, K.A., Spark plasma sintering of TiNi nano-powder. *Scr. Mater.*, 52 (2005) 455–460.
- [3] Whitney, M., Corbin, S.F., Gorbet, R.B., Investigation of the mechanisms of reactive sintering and combustion synthesis of NiTi using differential scanning calorimetry and microstructural analysis. *Acta Mater.*, 56 (2008) 559–570.
- [4] Shabalovskaya, S.A., On the nature of the biocompatibility and on medical applications of NiTi shape memory and superelastic alloys, *Bio-Medical Materials and Engineering*, 6 (4) (1996) 267-289.
- [5] Bansiddhi, A., Sargeant, T. D., Stupp, S. I., Dunand, D. C., Porous NiTi for bone implants: A review, *Acta Biomaterialia*, 4 (2008) 773–782.
- [6] Entchev, P.B. and Lagoudas, D.C., Modeling of transformation-induced plasticity and its effect on the behavior of porous shape memory alloys. Part II: porous SMA respons. *Mechanics of Materials*, 36(9) (2004) 893-913.
- [7] Nemat-Nasser, S., Su, Y., Guo, W.G. and Isaacs, J., Experimental characterization and micro-mechanical modeling of superelastic response of a porous NiTi shape-memory alloy. *Journal of the Mechanics and Physics of Solids*, 53(10) (2005) 2320-2346.
- [8] Liu, B., Dui, G., Zhu, Y., On phase transformation behavior of porous Shape Memory Alloys, *Journal of the mechanical behavior of biomedical materials*, 5 (2012) 9-15.
- [9] Qidwai, M.A., Entchev, P.B., Lagoudas, D.C., De Giorgi, V.G., Modeling of the thermomechanical behavior of porous shape memory alloys. *Int. J. of Solids Struct.*, 38 (48-49) (2001) 8653–8671.
- [10] Entchev, P.B., Lagoudas, D.C., Modeling porous shape memory alloys using micromechanical averaging techniques, *Mechanics of Materials*, 34 (1) (2002) 1–24.
- [11] Zhao, Y. and Taya, M., Analytical Modeling for Stress-Strain Curve of a Porous NiTi. *Journal of Applied Mechanics*, 74(2) (2007) 291-297.
- [12] Zhu, Y., Dui, G., A model considering hydrostatic stress of porous NiTi shape memory alloys, *Acta Mechanica Solida Sinica*, 24 (4) (2011).



- [13] Panico, M., Brinson, L.C., Computational modeling of porous shape memory alloys, *Int. J. Solids Struct.*, 45 (2008) 5613–5626.
- [14] Souza A.C., Mamiya E.N., Zouain N., Three-dimensional model for solids undergoing stress-induced phase transformations, *European Journal of Mechanics A/Solids*, 17 (1998) 789-806.
- [15] Auricchio, F., Petrini, L., A three-dimensional model describing stress-temperature induced solid phase transformations: solution algorithm and boundary value problems, *Int. J. for Numer. Meth. Eng.*, 61 (2004) 807–836.
- [16] Evangelista, V., Marfia, S., and Sacco, E., Phenomenological 3D and 1D consistent models for shape memory alloy materials, *Comput. Mech.*, 44 (2009) 405-421.
- [17] Lemaitre, J., Chaboche, J., *Mecanique des materiaux solides*, Dunod, Paris, (1988).
- [18] Suquet, P., Elements of homogenization for inelastic solid mechanics. In: *Homogenization techniques for composite media* (edited by E. Sanchez-Palencia and A Zaoui). Lecture Notes in Physics Vol. 272. Springer, Berlin, (1987) 194–275.
- [19] Luciano, R., Sacco, E., Variational methods for the homogenization of periodic heterogeneous media. *European Journal of Mechanics A/Solids*, 17-4 (1998) 599-617.
- [20] Greiner, C., Oppenheimer, S.M., Dunand, D.C., High strength, low stiffness, porous NiTi with superelastic properties. *Acta Biomaterialia* 1 (2005) 705–716.
- [21] Imwinkelried, T., Mechanical properties of open-pore titanium foam. *Journal of Biomedical Materials Research Part A*, 81(4) (2007) 964-970.
- [22] Xiong, J.Y., Li, Y.C., Wang, X.J., Hodgson, P.D, Wen, C.E., Titanium–nickel shape memory alloy foams for bone tissue engineering. *Journal of the mechanical behavior of biomedical materials I* (2008) 269-273.
- [23] Wang, X., Y. Li, et al., Porous TiNbZr alloy scaffolds for biomedical applications. *Acta biomaterialia*, 5(9) (2009) 3616-3624.
- [24] Wen, C.E., Xiong, J.Y., Li, Y.C. and Hodgson, P.D., Porous shape memory alloy scaffolds for biomedical applications: a review. *Phys. Scr. T139* (2010).